Effect of Bending-Twisting Coupled Deformation on Pure Bending Strength and Fracture Morphology of CFRP Angle-Ply Laminate

Kazuki Terasaki[1*], Kiyotaka Obunai[2], Kazuya Okubo[3]

[1] Graduate School of Doshisha University, Kyotanabe, Kyoto, Japan
[2] Department of Mechanical Engineering, Doshisha University, Kyotanabe, Japan.
[3] Department of Mechanical Engineering, Doshisha University, Kyotanabe, Japan.

* Corresponding author. Tel.: 080-3945-1390; email: ctwf0580@mail4.doshisha.ac.jp
Manuscript submitted December 25, 2021; accepted January 25, 2022.
doi: 10.17706/ijmse.2022.10.4.88-95.

Abstract: The purpose of this study is to investigate the effect of bending-twisting coupled deformation on the bending strength of CFRP in which laminate configuration has symmetricity and angled fiber orientation. In this study, a novel type of test fixture for the pure bending test that permits the coupled bending-twisting deformation is newly developed for the pure bending test. Test results showed that the pure bending strength of the angle-ply laminates was decreased when bending-twisting coupled deformation was permitted. The normalized bending strength when bending-twisting coupled deformation is permitted was decreased with the increase of coupled component of angle-ply laminate. Observations of fracture morphology of specimen also showed that the specimen was firstly failed at the 0° layer on the compression side no matter if the coupled deformation was permitted or constrained. However, when the coupled deformation was permitted, the failure was occurred at lower applied bending stress compared with when coupled deformation was constrained. Moreover, when the coupled deformation was permitted, the failure of the 0° layer has occurred at the diagonal portion of the specimen. These results suggested that the existence of in-plane shear stress at 0° layer affects the fracture morphology of the specimen.

Key words: CFRP, angle-plied laminate, bending-twisting coupling deformation, pure bending, Classical laminate theory.

1. Introduction

Carbon fiber-reinforced plastics (CFRP) have been widely used in a variety of fields, where not only require high strength but also require weight reduction, such as aircraft and space structures [1], [2]. For satisfying the requirements, the configuration of CFRP should be well designed for individual applications. Especially, when using resin-impregnated carbon fiber lamina called "Prepreg", the major objective of designing is to determine the optimal laminate configuration i.e., optimal combinations of fiber orientations in the structures under assumed loading conditions. By controlling the fiber orientations in the CFRP, the apparent mechanical property of structures can be designed for their applications [3], [4]. It is well known that, when the fiber orientation has specific combinations, the coupled deformation of structures has occurred [5], [6]. This coupling effect of deformation is sometimes effectively utilized, for example, to suppress the "divergence" of wing structures [7] or to control the twist angle of the tilt-rotor blade [8]. However, there are few studies have been discussed how to affect these coupling deformations on the strength of structures. Moreover, there

are no standardized material tests that permit the coupled deformation during testing. Therefore, the purpose of this study is to investigate the effect of bending-twisting coupling deformation on the bending strength of CFRP in which laminate configurations have symmetricity and angled fiber orientation. In this study, a novel type of test fixture for pure bending test that permits the coupled bending-twisting deformation is newly developed. By controlling the rotational degrees of freedom of the test fixture, the coupled torsional deformation of the specimen was permitted or constrained. The effect of coupled deformation on the fracture morphology of CFRP laminates was also investigated.

2. Materials and Experimental Methods

2.1. Materials

A unidirectional carbon fiber/epoxy prepreg sheet (Toho Tenax Co., Ltd., tensile modulus: 137 GPa, tensile strength: 2060 MPa, fiber volume content: 60%) was used as the material. Prepreg sheets were laminated in the specified configurations, and these were pre-cured at a temperature of 80°C and a pressure of 0.05 MPa for 25 minutes using a heat press. After that, the temperature and applied pressure were changed to 130°C and 0.5 MPa then kept 80 minutes to fabricate the laminates. For the tensile test, a four-layer of the unidirectional laminate was fabricated to prepare the strip-shaped specimen (200 ×25 ×0.8 mm^3). For the pure bending test, $[0/\theta_5/0]$ of angle-plied symmetric laminates were also prepared to fabricate the strip-shaped specimen ($100\times40\times2mm^3$).

2.2. Tensile Test

The three types of specimens in which fiber orientation against the longitudinal direction of the specimen was 0, 45, and 90° were prepared to investigate the apparent elastic modulus and Poisson's ratio along the longitudinal direction of the specimen. The strains of the specimen during the tensile test were measured by strain gauges adhered to the specimen. The measured elastic constants of unidirectional laminae were used to calculate the elastic constants of angle-plied symmetric laminates based on classical laminate theory. Here, the relationship between applied force and deformation at angle-plied symmetric laminates was written out in the matrix notation as follows.

$$\begin{pmatrix} Nx \\ Ny \\ Nxy \\ Mx \\ My \\ Mxy \end{pmatrix} = \begin{pmatrix} A_{11} & A_{12} & A_{16} & B_{11} & B_{12} & B_{16} \\ A_{12} & A_{22} & A_{26} & B_{12} & B_{22} & B_{26} \\ A_{16} & A_{26} & A_{66} & B_{16} & B_{26} & B_{66} \\ B_{11} & B_{12} & B_{16} & D_{11} & D_{12} & D_{16} \\ B_{12} & B_{22} & B_{26} & D_{12} & D_{22} & D_{26} \\ B_{16} & B_{26} & B_{66} & D_{16} & D_{26} & D_{66} \end{pmatrix} \begin{pmatrix} \varepsilon_{x0} \\ \varepsilon_{y0} \\ \gamma_{xy0} \\ \chi_x \\ \chi_y \\ \chi_{xy} \end{pmatrix} \quad (1)$$

$$D_{ij} = (1/3) \sum_{k=1}^{n} \left(\overline{Q_{ij}}\right)_k \left(z^3{}_k - z^3{}_{k-1}\right)$$

$$\chi_{xy} = D'_{16} Mx \quad (2)$$

For considering the coupled deformation between bending and torsion, the component of the stiffness tensor D'_{16} was calculated for each laminate configuration.

2.3. Pure Bending Test

Fig. 1 shows a schematic illustration of the test fixture for the pure bending test. The test fixture has two rotational degrees of freedom around axis A and B as shown in the figure. These axes are equipped with bearing to minimize the friction against rotation. The specimen was gripped by a test fixture and unidirectional displacement along the y-axis was applied by an electro-hydraulic servo fatigue testing machine. When the coupled deformation of the specimen is constrained, the rotation around axis A was fixed

by a support block fastened by screws as shown in the figure at "Fixed". According to the applied displacement, the bending moment was applied to the specimen. Due to the bending deformation of the specimen, the test fixture was rotated around axis B. On the other hand, when the coupled deformation of specimen is permitted, the rotational degree of freedom around both axes was set to be free as shown in the figure at "Torsional". Therefore, due to the bending deformation of the specimen, the test fixture was not only rotated around axis B, but also rotate around axis A. The apparent bending stress at the center of the specimen was calculated by the following equation.

$$\sigma_b = \frac{P}{Z} l_m = \frac{P}{Z}\left\{ l_x \cos\phi + l_y \cos\phi + \frac{L}{2\phi}(1 - \cos\phi) \right\} \tag{3}$$

Here, the large deflection of the specimen was considered to calculate the bending stress of the specimen. Where Z is the section modulus of the specimen, and l_x and l_y are the distances in the x- and y-directions from axis B to the specimen. P and ϕ denote the applied force, the rotation angle of the test fixture around axis B. The rotation angle of the test fixture around axis B was measured by a rotary encoder attached to the test fixture. The twist angle of the gripped part around axis A was also measured by a laser displacement meter. In this study, four types of specimens in which the orientation of angle-plied fiber against the longitudinal direction of the specimen was 0, 20, 30, and 40° were prepared. The applied displacement speed was set to be 0.5 mm/min, and at least 4 specimens were tested.

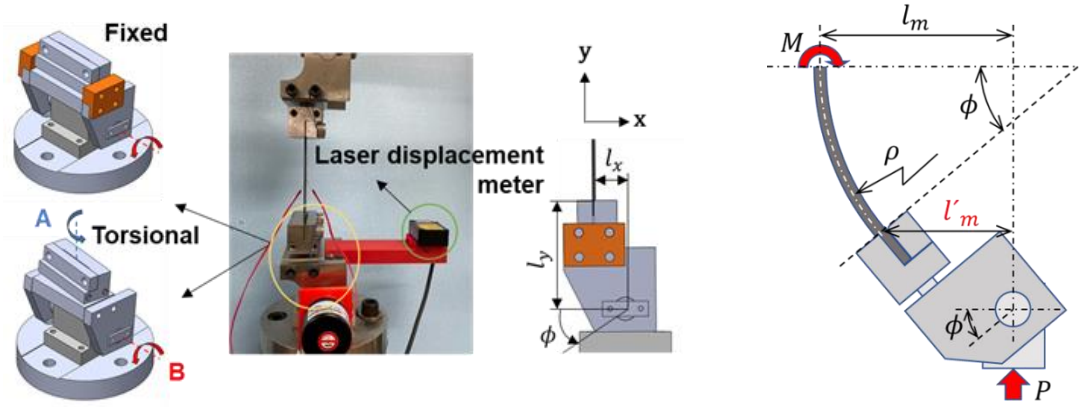

Fig. 1. Schematic illustration of the test fixture for the pure bending test.

3. Result and Discussions

3.1. Pure Bending Test Results

Fig. 2 shows a typical bending stress-bending strain diagram of $[0/30_5/0]$ angle-ply laminate subjected to pure bending load. Fig. 2(a) shows a result of the pure bending test while bending-twisting coupled deformation was constrained. Fig. 2(b) also shows a result of the pure bending test when bending-twisting coupled deformation was permitted. Here, the apparent bending stress was calculated at the center of the specimen by using equation (3). Test results showed that no matter if the bending-twisting coupled deformation was permitted or constrained, the apparent bending stress was almost linearly increased with the increase of bending strain until the failure. Moreover, when the bending-twisting coupled deformation was permitted, the twist angle of the specimen was almost linearly increased with the increase of apparent bending stress. Test results showed that the apparent bending strength of the specimen was decreased when the bending-twisting coupling deformation was permitted. Fig. 3 also shows an apparent bending strength of the specimen with respect to the fiber orientation angle of the angle-ply layer. Test results showed that the bending strength of both conditions was decreased with the increase of lamination angle. Moreover, the

bending strength of the "Torsional" condition was always decreased compared with that of the "Fixed" condition, if the fiber orientation of the angle-ply layer exceeds 0°.

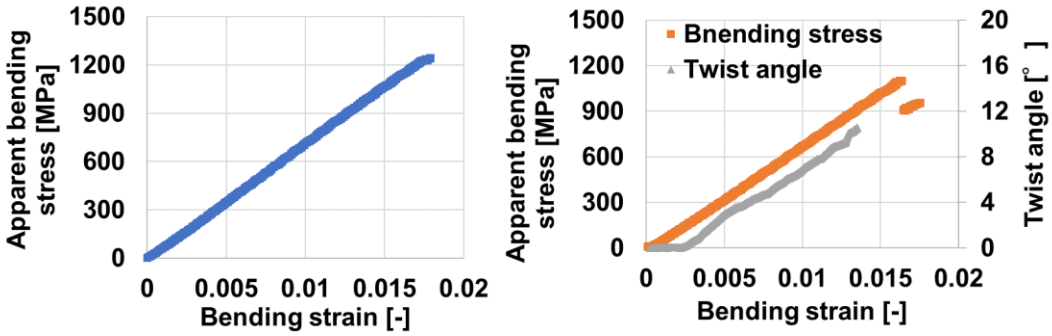

(a)"Fixed" condition (b)"Torsional" condition

Fig. 2. Typical bending stress-bending strain curves of $[0/30_5/0]$ CFRP specimen.

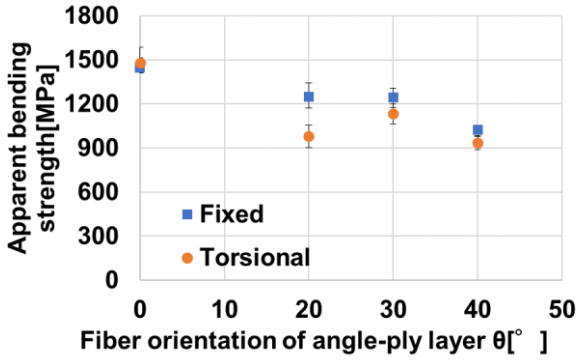

Fig. 3. Apparent bending strength of the specimen with respect to fiber orientation of angle-ply layer.

The compressive failure of the specimen was occurred around the grip part of the specimen, no matter if the bending-twisting coupled deformation was permitted or constrained. To discuss the actual bending strength of the specimen, the compressive bending stress just acting on the failure portion was calculated by the following equation. When bending-twisting coupling deformation was permitted, the change of moment arm length due to twisting was considered.

$$\sigma'_{b-Tors} = \frac{P}{Z} l'_{m-Tors} = \frac{P}{Z}\left\{l_x \cos\phi + l_y \cos\phi + \frac{B}{2} sin\phi sin\gamma\right\} \quad (4)$$

$$\sigma'_{b-Fix} = \frac{P}{Z} l'_{m-Fixed} = \frac{P}{Z}\{l_x \cos\phi + l_y \cos\phi\} \quad (5)$$

Here, γ denote the twist angle of the test fixture around axis A. Fig.4 shows the normalized bending strength and twist angle at the failure of specimens with respect to the component of stiffness tensor of angle-ply laminate. Here, the bending strength of the "Torsional" condition was normalized by dividing that of the "Fixed" condition. Test results showed that the normalized bending strength of $[0/20_5/0]$ and $[0/30_5/0]$ laminates were decreased with the increase of coupled components. However, the normalized bending strength was degraded at $[0/20_5/0]$ compared to that of $[0/40_5/0]$, even if these have almost the same coupled components. The twist angle of the specimen was also showed that when the coupling components have existed, the twist deformation has occurred. However, the twist angle of the specimen was not simply related to the coupling components of the stiffness tensor. These results suggested that the normalized bending strength and twist angle of angle-ply laminate could not be explained by the tendency of coupled components of stiffness tensor.

Fig. 4. Normalized bending strength and twist angle with respect to the component of stiffness tensor of angle-ply laminate.

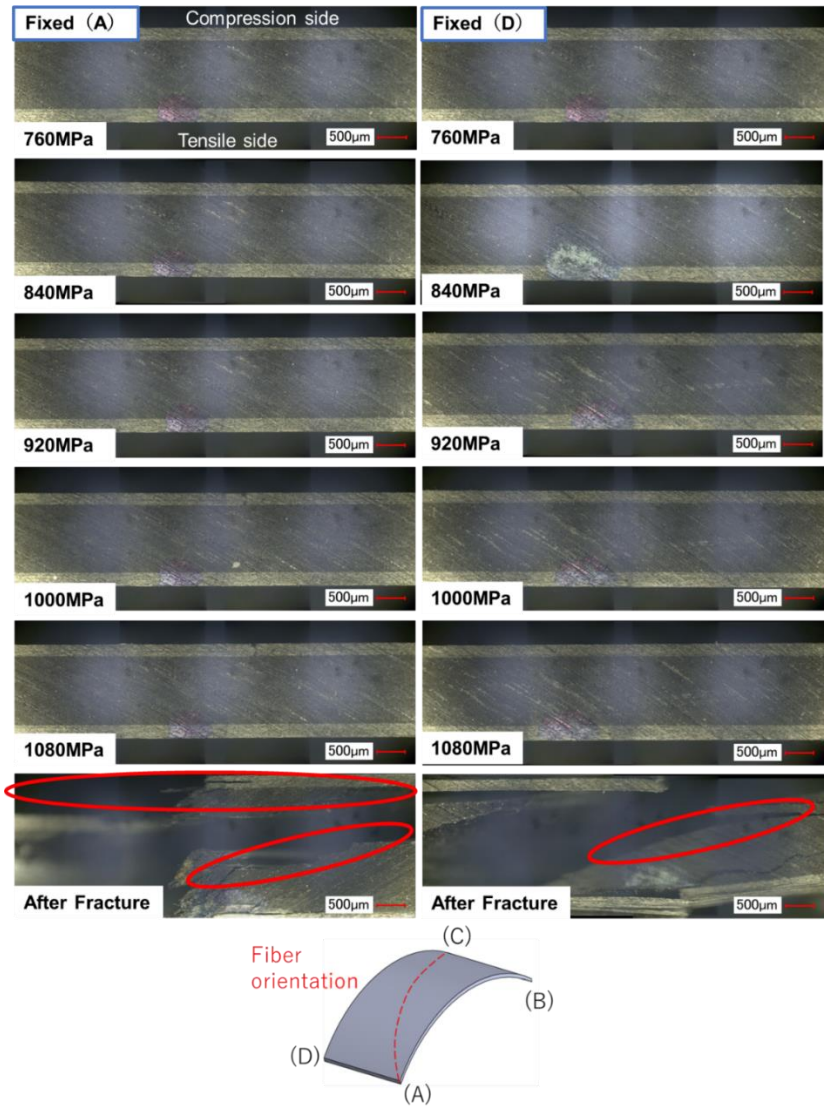

Fig. 5. Typical observation results of [0/30$_5$/0] laminates under "Fixed" condition.

3.2. Observations of Specimen during Bending Test

The damage morphology of the specimen during the pure bending test was observed from the side by optical microscope. To clarify the progress of damage, the observation was conducted every 80 MPa of bending stress increment. Fig.5 and 6 show the typical observation results of [0/30$_5$/0] laminates. Fig.5

shows the observation results of the “Fixed” condition. Fig.6 also shows the observation results of the “Torsional” conditions. Here, the observation was conducted around the upper gripped part from both corners (A) and (D) of the specimen as shown in the schematic illustration. Observation results showed that the damage of specimens was firstly occurred at the compression side of 0° layer, no matter if coupling deformation was constrained or permitted. However, failure of 0° layer was only observed at one side of the specimen as can be seen in Fig. 6(A), when coupling deformation was permitted. On the other hand, when coupling deformation was constrained, the failure occurred through both sides of the specimen. Comparing the magnitude of bending stress when failure of 0° layer has occurred, the bending stress of the "Torsional" condition was decreased compared with that of the "Fixed" condition. Moreover, the diagonal corners of the "Torsional" specimen where the failure of 0° layer was confirmed were almost coincident with the fiber direction of angle-ply layers.

Due to the existence of the fiber in the diagonal direction of the specimen, the curvature of the specimen was increased along the fiber direction. Therefore, the length of the moment arm at the corner (A) was increased compared with that of the corner (D). As a result, when the twisting deformation of the specimen was permitted, the failure only occurred at one side of the specimen.

Fig. 6. Typical observation results of $[0/30_5/0]$ laminates under “Tortional” condition.

3.3. Damage Morphology of Specimen

From the above discussions, when the bending-twisting coupling deformation was permitted, the failure of the 0° layers occurred in comparatively lower bending stress. Fig.7 shows the schematic illustrations of damage morphology during the pure bending test. No matter if the coupled deformation was permitted or constrained, the compressive failure was occurred only in the diagonal corner of the specimen, due to the

existence of the angle-ply layer. However, when coupled deformation was permitted, the torsional deformation of the specimen is also occurred due to the bending deformation. Due to this torsional deformation, the in-plane shear stress has occurred at 0° layer at the "Torsional" condition. Therefore, both bending stress and in-plane shear stress were existing at the compression side of the specimen. Because of this combined stress condition, the compressive failure of 0° layer might have occurred in comparatively lower bending stress.

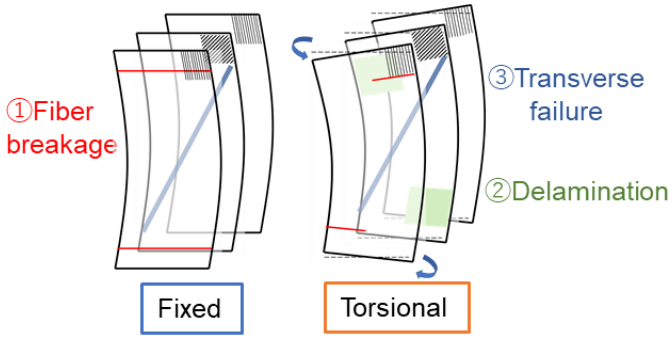

Fig. 7. Schematic illustrations of damage morphology during pure bending test.

4. Conclusions

(1) The normalized bending strength and the twist angle of angle-ply laminate could not be explained by the tendency of coupled components of stiffness tensor.

(2) Because of the bending-twisting deformation of the specimen, the length of the moment arm is not coincident with both sides in the width direction of the specimen. Therefore, the failure of the specimen only occurred on one side of the specimen.

(3) Because the combined stress condition occurred due to the bending-twisting coupling deformation, the in-plane compressive stress along the fiber direction of the 0° layer may be increased compared with when the coupled deformation was constrained.

Conflict of Interest

The authors declare no conflict of interest.

Author Contributions

All authors conducted the research; Kazuki Terasaki and Kiyotaka Obunai analyzed the data and wrote the paper; all authors had approved the final version.

Acknowledgment

This work was partly supported by JSPS KAKENHI Grant Number 21K03779.

References

[1] Christopher, B., Reda, J., A, V., & Rob, H. (2017). Composites stacking sequence optimization for aeroelastically tailored forward-swept wings. *Struct Multidisc Optim*.

[2] Shun, T., Tadashige I., & Atsuhiko S. (2016). Sensitivity analysis of thermal deformation of CFRP laminate reflector due to fiber orientation error. *Journal of Mechanical Science and Technology, 30(10)*.

[3] Ylva, L., & Malin, A. (2014). In-plane deformation of multi-layered unidirectional thermoset prepreg – Modelling and experimental verification. *Composites: Part A 56*.

[4] Naghipour, P., Bartsch, M., Chernova, L., Hausmann, J., & Voggenreiter, H. (2010). Effect of fiber angle orientation and stacking sequence on mixed mode fracture toughness of carbon fiber reinforced plastics: Numerical and experimental investigations. *Materials Science and Engineering A, 527*.

[5] Ikuma I., Kenta K., *et al.* (2018). *Civil Engineering Society Paper Series A2, 74(2)*.

[6] Hiroki, S., Takashi, M., &Toshiro, H. (2012). *Civil Engineering Society Paper Series A2, 68(1)*.
[7] Stodieck, O., Cooper, J. E., Weaver, P. M., & Kealy, P. (2015). Optimization of tow-steered composite wing laminates for aeroelastic tailoring. *AIAA JOURNAL, 53(8)*.
[8] Peng, L., Sebastien, P., Fazila, M.-Z., *et al.* (2015). Performance improvement of small-scale rotors by passive blade twist control. *Journal of Fluids and Structures, 55*.

Kazuki Terasaki was born in Fukuoka, Japan on November 22, 1997. He is majoring in Department of Materials Engineering at Graduate School of Doshisha University, Kyotanabe, Kyoto, Japan.

Kiyotaka Obunai joined the Department of Mechanical and Systems Engineering at Doshisha University as an associate professor in 2018. His research areas include mechanics of materials, mechanics of composites materials, and materials modeling.

Dr. Kazuya Okubo joined the Department of Energy and Mechanical Engineering at Doshisha University as a professor in 2003. His research areas include mechanics of materials, mechanics of composites materials, and damage and fracture mechanics.